Carbohydrate Polymers 95 (2013) 621–629

Contents lists available at SciVerse ScienceDirect

Carbohydrate Polymers

journal homepage: www.elsevier.com/locate/carbpol

Thermal characterization and detailed kinetic analysis of *Cassava* starch thermo-oxidative degradation

Bojan Janković*

Faculty of Physical Chemistry, Department for Dynamics and Matter Structure, University of Belgrade, Studentski trg 12-16, P.O. Box 137, 11001 Belgrade, Serbia

ARTICLE INFO

Article history:
Received 15 December 2012
Received in revised form 7 March 2013
Accepted 9 March 2013
Available online 15 March 2013

Keywords:
Cassava starch
Thermo-oxidative degradation
Complex system
Kinetic parameters
"Lumped" model
Mechanistic scheme

ABSTRACT

Detailed kinetic analysis of *Cassava* starch thermo-oxidative degradation was performed, using thermogravimetric analysis (TGA) and derivative thermogravimetry (DTG) at four different heating rates. It was found that degradation process is very complex, as identified through continuous change of apparent activation energy with degree of degradation. It was established that process proceeds through three main degradation stages with one additional sub-stage attached to the second degradation stage, which was detected by appearance of "shoulder" on DTG curves. It was found that most important degradation stage can be described by "lumped" model, which implies that free radicals simultaneously attack both linear and branched molecular forms of the starch. This is characterized by an unusually high value of obtained reaction order ($n = 3.49$). Application of nonlinear least squares method was confirmed the reliability of evaluated kinetic parameters and function of reaction mechanism, which were derived on the basis of other kinetic methods.

1. Introduction

Starch is the form of carbohydrate reserve in nearly all green plants and it is the major carbohydrate component in food (Van den, 1981). On the industrial scale, starch is isolated from seeds of cereal grains (corn, wheat, rice), tubers (potato), roots (tapioca, sweet potato) and the pith of the tapioca palm (Swinkels, 1985).

Starch granules consist of two structurally and functionally very different polymers: amylose and amylopectin. Starch functionality depends on the average molar mass of amylose and amylopectin as well as on their molecular structure and organisation within the granule. The amylose contents of most starches, such as barley, wheat, oat, maize and potato starch, are all in the range of 20–30% (Morrison & Laignelet, 1983; Morrison, Law, & Snape, 1993). In amylomaize starch, the amylose content is higher (about 50–80%) and in the waxy starches very low (<1%) (Morrison & Laignelet, 1983). Amylose is an essentially linear polymer composed of α-D-glycopyranose units linked through α-(1 → 4) linkages. Amylopectin is a highly branched polymer; 5% of its structure is α-(1 → 6) branch links (Ball, 1996).

Cassava (*Manihot esculenta*, Crantz) is one of the most important starchy tubers in tropical zones, with 167 million tones of fresh tuber and roots produced annually all over the world (FAO, 1994). Being very rich in starch (90% of the dry matter), *Cassava* is mainly used in traditional human foods after more or less elaborate processing, e.g. chickwangue, gari, farinha de mandioca, but is also used industrially for the production of starch and starch derivatives, e.g. dextrins and glucose (Greenwood & Milne, 1968). As traditional and industrial *Cassava* uses often implies a thermal processing step, knowledge of the starch granule modifications occurring during cooking is essential to improve the sensory and nutritional properties of subsequent starch-based foods. Among the starchy staples, *Cassava* gives a carbohydrate production which is about 40% higher than rice and 25% superior to corn, with the result that *Cassava* is the cheapest source of calories for both human nutrition and animal feeding. Typical composition of *Cassava* root is moisture (70%), starch (24%), fiber (2%), protein (1%) and the other substances including minerals (3%) (Tonukari, 2004).

There have been several reports of the studies of the degradation features of the starch from different sources analyzed by thermal analysis techniques (Ji et al., 2003; Morita, 1956, 1957; Tian, Xu, Xie, Zhao, & Jin, 2011). However, in the literature there are very few papers related to the detailed degradation kinetics of various types of starch (as A-, B-, and C-type starches (Bogracheva, Wang, Wang, & Hedley, 2002)) (Guinesi et al., 2006; Pielichowski, Tomasik, & Sikora, 1998; Pineda-Gómez, Coral, Ramos-Rivera, Rosales-Rivera, & Rodríguez-García, 2011). It should be noted that the published results are mainly based on the phenomenological (*empirical*) kinetic equations (Guinesi et al., 2006). In the scientific literature there are no published results based on a comprehensive

* Tel.: +381 11 2187 133; fax: +381 11 2187 133.
E-mail address: bojanjan@ffh.bg.ac.rs

0144-8617/$ – see front matter © 2013 Elsevier Ltd. All rights reserved.
http://dx.doi.org/10.1016/j.carbpol.2013.03.038

detailed kinetic analysis of *Cassava* starch degradation under the non-isothermal conditions, with the provided detailed mechanistic scheme of the whole process.

In order to understand more precisely the overall degradation mechanism of *Cassava* starch granules during thermal exposure at the elevated temperatures under controlled linear heating, the combined "*stationary point*" and "*model-free*" kinetic approaches (Adnađević, Janković, Kolar-Anić, & Minić, 2007; Burnham & Dinh, 2007; Vyazovkin & Wight, 1999) were used in this study. For the investigated degradation process, the applied kinetic pathways are carefully compared, by introducing the specific statistical tests. Statistical tests were introduced in order to determine the reliable kinetic mechanism. In addition, the objective of this paper is also to give a detailed presentation of the methodology used and to provide some important kinetic clues for the thermo-oxidative degradation of *Cassava* starch, as very significant source of carbohydrates.

2. Materials and methods

2.1. Extraction of Cassava starch

An original commercial packaging of fresh *Cassava* roots (1 set with 500 g of *Cassava* roots) was supplied by Nanning China Tropical Agricultural Machinery Company, Ltd. (Nanning, Guangxi, China). *Cassava* roots were washed, peeled, milled, sieved and the mash was washed. The solid residue was retained in the sieve (250 mesh) and the suspension kept within 2 h decanting. Then, the starch was filtered, washed and dried in an oven at 40 °C. The obtained *Cassava* starch was maintained in a desiccator over the anhydrous calcium chloride, until the constant mass. The moisture content of starch is within 20% of moisture level recommended for extraction of starch from commercial sources (Soni, Sharma, Dun, & Gharia, 1993).

2.2. Thermo-analytical measurements

Thermogravimetic (TG) and derivative thermogravimetric (DTG) curves were recorded using a simultaneous TGA-DTA SDT 2960 device (TA Instruments) (TA Instruments, 159 Lukens Drive, New Castle, DE 19720), under an air flow at 100 mL min^{-1} and at a heating rates of β = 10, 20, 30 and 40 °C min^{-1}. Thermo-analytical experiments were carried out in the temperature range of T = 20–600 °C. Heating the sample in the specified temperature range was carried out with the aim of concentrating on the study of chemical structure changes of starch, during thermal degradation in oxidative atmosphere. Sample portions with approximately of $m \approx 10$ mg were used for thermogravimetric measurements. Alumina crucibles were used for all thermo-analytical experiments. Mass calibrations were realized according the manufacturer specifications and an empty alumina crucible was used as reference. TG measurements on each of the given heating rate was repeated twice due to the stability and reproducibility of the obtained thermo-analytical data.

3. Theoretical background

In general, a typical kinetic equation for the investigated process can be expressed as (Chiangga, Suwannasopon, & Trivijitkasem, 2012):

$$\frac{d\alpha}{dt} = A \times \exp\left(-\frac{E_a}{RT}\right) f(\alpha) \quad (1)$$

where $d\alpha/dt$ is degradation rate [min^{-1}], A is the pre-exponential (frequency) factor [min^{-1}], E_a is the apparent activation energy [J mol^{-1}], R is the gas constant [8.314 J K^{-1} mol^{-1}], T is the absolute temperature [K], and $f(\alpha)$ is the function of α (α is the degree of degradation: $\alpha = (m_o - m_T)/(m_o - m_f)$, where m_o, m_T and m_f are the initial, actual and final mass of the sample, respectively) depends on the particular degradation mechanism.

If the temperature of a sample is changed by a constant value of β (linear heating rate) ($\beta = dT/dt$), the variation of the degree of degradation can be analyzed as a function of temperature. Therefore, the reaction rate gives:

$$\frac{d\alpha}{dt} \equiv \beta \times \frac{d\alpha}{dT} = A \times \exp\left(-\frac{E_a}{RT}\right) f(\alpha) \quad (2)$$

Separating the variable and rearranging and integrating Eq. (2), it can be obtained:

$$g(\alpha) = \int_0^\alpha \frac{d\alpha}{f(\alpha)} = \frac{A}{\beta} \int_{T_0}^{T} \exp\left(-\frac{E_a}{RT}\right) dT \quad (3)$$

where $g(\alpha)$ is integral form of reaction mechanism function, and T_0 is starting temperature of the non-isothermal experiment. Eq. (3) cannot be expressed by a simple analytical form since its right-hand side corresponds to a series of infinite gamma functions. In mathematical practice, Eq. (3) can be expressed in the following form (Vyazovkin & Wight, 1998):

$$g(\alpha) = \frac{A}{\beta} \int_0^T \exp\left(-\frac{E_a}{RT}\right) dT = A \times \exp(-x) \times \left[\frac{T}{\beta}\pi(x)\right], \quad (4)$$

which was introduced an approximation for the lower limit of the integral on the right-hand side of Eq. (5) as $T_0 \to 0$, bearing in mind that value of temperature T_0 in practical cases is very low. Variable $x = E_a/RT$ is reduced apparent activation energy, while $\pi(x)$ represents an approximation of the temperature integral, which cannot be exactly calculated (Gyulai & Greenhow, 1973). However, the rational expression for $\pi(x)$ performed by Senum and Yang (Senum & Yang, 1977) gives sufficiently accurate approximation.

3.1. Isoconversional ("model-free") methods

By using the Coats–Redfern approximation for temperature integral (Coats & Redfern, 1964) to solve Eq. (3) and considering that $2RT/E_a$ is much lower than unity, the Kissinger–Akahira–Sunose (KAS) (Kissinger, 1957; Akahira & Sunose, 1971) equation can be written in the form:

$$\ln\left(\frac{\beta}{T^2}\right) = \ln\left[\frac{AR}{g(\alpha)E_a}\right] - \frac{E_a}{RT} \quad (5)$$

For each degree of degradation, the linear plot of $\ln(\beta/T^2)$ versus $1/T$ enables E_a and $\ln[AR/g(\alpha)E_a]$ to be determined from the slope and the intercept, respectively.

The isoconversional method suggested by Friedman (FR) (Friedman, 1964) is based on Eq. (2), in logarithmic form:

$$\ln\left[\beta\left(\frac{d\alpha}{dT}\right)\right] = \ln[Af(\alpha)] - \frac{E_a}{RT} \quad (6)$$

For a constant α, the plot of $\ln[\beta(d\alpha/dT)]$ versus. $1/T$ obtained from curves recorded at several heating rates, should be a straight line whose slope gives us the value of E_a. From the intercept of a given straight line ($\ln[Af(\alpha)]$), it is possible to determine the pre-exponential factor for each conversion value, only if the differential form of reaction model $f(\alpha)$, is known.

3.2. Stationary point (SP) kinetic approach

Stationary point (SP) method (Adnađević et al., 2007) is based on logarithmic form of Eq. (2), in relation to the fixed or specific points at the corresponding conversion rate curves, so it can be expressed as:

$$\ln\left(\frac{d\alpha}{dt}\right)_p = \ln\left[A \times f(\alpha)_p\right] - \frac{E_a}{RT_p} \quad (7)$$

where $(d\alpha/dt)_p \equiv \beta\,(d\alpha/dT)_p$ is the value of the maximum degradation rate at the peak temperature (T_p), $\ln[Af(\alpha)_p]$ is a "*solid*" constant at β = const. It is possible to calculate the value of E_a, from the slope of linear dependence $\ln(d\alpha/dt)_p$ versus $1/T_p$.

3.3. Estimation of the kinetic parameters by the nonlinear least squares method

In order to obtain the accurate values of the kinetic parameters, the nonlinear least squares estimation (NLE) method, was applied for degradation process of analyzed *Cassava* starch samples. For a given set of parameters, the basic kinetic law equation may be numerically integrated to give the corresponding α–T curve, in terms of $\alpha_{m,\mathrm{calc}}$. Then, the sum of squares of residuals (SSR) between the experimental ($\alpha_{m,\mathrm{exp}}$) and corresponding calculated ($\alpha_{m,\mathrm{calc}}$) conversion values, as defined by Eq. (8), is computed. The goal of the NLE method is to find the parameter values for which the *SSR* has a minimum value. In this case, method presented by Marquardt was used. The actual calculation was performed using optimization function of MATLAB® program (MathWorks Inc., 2012), based on Eq. (8):

$$\mathrm{SSR} = \sum\nolimits_m (\alpha_{m,\mathrm{calc}} - \alpha_{m,\mathrm{exp}})^2 \tag{8}$$

Subscript m in Eq. (8) represents the number of points used in the numerical calculations.

In this problem, fundamental equations containing unknown parameters are given by a nonlinear differential equation. The program provides a numerical solution of the differential equations and NLE. In practical optimization calculations, it is important to assign appropriate starting values to the unknown parameters. If the starting parameter values are set inappropriately, the iteration will not necessarily converge at optimal parameter values. Here, the suitable starting parameter values estimated through the stationary point method that uses the Arrhenius-like plot were implemented. The fit between observed and calculated values at the obtained parameters is given in percentage of the highest observed α value, $\alpha_{\mathrm{exp}}^{\mathrm{max}}$:

$$\mathrm{fit}\ [\%] = \frac{\sqrt{\mathrm{SSR}/N}}{\alpha_{\mathrm{exp}}^{\mathrm{max}}} \times 100\% \tag{9}$$

where N is the total number of data in conversion curve. Method actually tests the error between observed (experimental) and calculated values. Therefore, the output fit [%] is also referred as "*deviation* (%)" (Varhegyi, Antal, Szekely, & Szabo, 1989).

3.4. Determination of the reaction mechanism

The combination's of Eqs. (2) and (4) leads to one of two new functions, $z(\alpha)$, in the non-isothermal conditions:

$$z(\alpha) = \left(\frac{d\alpha}{dt}\right) \times \left[\frac{T}{\beta}\pi(x)\right] = f(\alpha)g(\alpha). \tag{10}$$

Recently, it was found that the term $[T/\beta\cdots\pi(x)]$ in Eq. (10) is proportional to T^2 (Málek, 1992). Therefore, a simplified expression for $z(\alpha)$ function is approximated as:

$$z(\alpha) \approx \left(\frac{d\alpha}{dt}\right) \times T^2 \tag{11}$$

One can easily transform experimental data to the $z(\alpha)$ function by using Eq. (11) and then normalize $z(\alpha)$ within the (0,1) interval. Another new function, $y(\alpha)$, can be defined as (Málek, 1992):

$$y(\alpha) = \left(\frac{d\alpha}{dt}\right) \times \exp(x) = A \times f(\alpha) \tag{12}$$

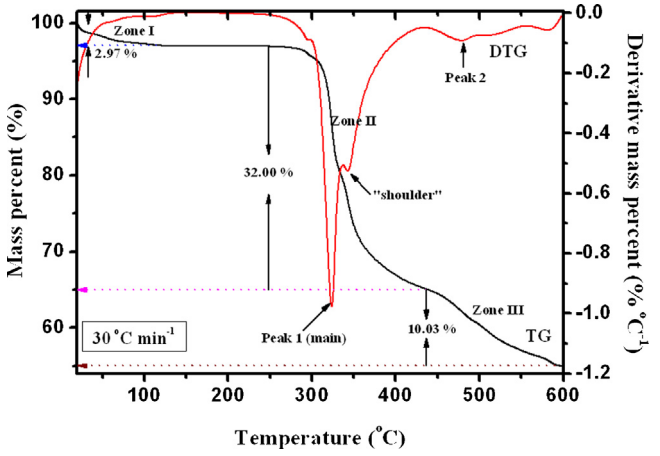

Fig. 1. The TG–DTG curves of the non-isothermal thermo-oxidative degradation process of *Cassava* starch samples, recorded on the heating rate of 30 °C min^{-1}.

The $y(\alpha)$ function is also usually normalized within (0,1) interval. Two important parameters α_m and α_P^{∞}, at which the functions $y(\alpha)$ and $z(\alpha)$ have a maximum, respectively, are normally calculated by mathematical software. Then, function $f(\alpha)$ is determined through the schematic kinetic diagram introduced by Málek (Málek, 1992; Málek, Mitsuhashi, & Criado, 2001).

4. Results and discussion

4.1. Thermal stability

TGA has proved to be a suitable method to investigate the thermal stability of different organic compounds especially for carbohydrate polymers (Rahman, Sin, Rahmat, & Samad, 2010). The knowledge of degradation and the mode of decomposition under the influence of heat are highly recommended in the processing optimization. The study of the kinetics of the different decomposition processes may help in the identification of the degradation mechanisms.

The thermogravimetric (TG) and the corresponding derivative (DTG) curves for the degradation process of *Cassava* starches at 30 °C min^{-1} are shown in Fig. 1.

TG and DTG curves show three main zones (designated by Zone I, II and III (Fig. 1)) in degradation process of *Cassava* starches. As it is clear from Fig. 1, the sample revealed the conspicuous difference in degradation behavior during Zone II of the DTG curve. Marked zones indicate three steps in mass loss. First mass loss was between 25 and 112 °C (2.97%; Zone I), which is attributed to dehydration that occurs in a single step. After dehydration, the investigated sample is stable up to 248 °C and above this temperature we can see that thermal degradation occurs in probably two overlapping steps (Fig. 1; Zones II (32.00%) and III (10.03%)) between 248 and 585 °C. It should be noted that in second zone, which belongs to the main degradation stage (the principal decomposition process of *Cassava* starch) we can see a sharp and well-defined peak (Peak 1 (main) on DTG curve; Fig. 1). However, with increasing of temperature, this peak shows asymmetric "deformation to the right", with the appearance of "shoulder". This phenomenon was detected at all considered heating rates. This effect indicates that the main degradation stage itself is quite complex, and it probably contains one sub-stage which is precisely defined by the appearance of "shoulder". Just beyond Zone II, Zone III below, which is characterized by the much broader ("diffusion") peak (with a less intensity) (Peak 2), at the higher temperatures (Fig. 1). In the case of anhydrous sample, the complex second degradation stage (Zone II) probably involves one reaction step and one prolonged reaction sub-step

Table 1
The values of characteristic temperatures (T_{p1}, T_{psh} and T_{p2}) observed for the first and second peaks (numbered 1 and 2) as well as for "shoulders" on the corresponding DTG curves, in the case of thermo-oxidative degradation of *Cassava* starch samples; the values of degradation rates ($(d\alpha/dt)_{p1}$, $(d\alpha/dt)_{psh}$ and $(d\alpha/dt)_{p2}$) and the residual mass loss (Δm) are also given.

β (°C min^{-1})	Peak 1 (main)		"Shoulder" (sh)		Peak 2		Δm (%)
	T_{p1} (°C)	$(d\alpha/dt)_{p1}$ (min^{-1})	T_{psh} (°C)	$(d\alpha/dt)_{psh}$ (min^{-1})	T_{p2} (°C)	$(d\alpha/dt)_{p2}$ (min^{-1})	
10	329.04	0.22636	342.63	0.17781	481.82	0.02075	42.95
20	331.57	0.48655	345.26	0.28094	489.70	0.03712	43.75
30	333.55	1.28081	347.24	0.43365	494.95	0.06819	45.00
40	335.52	1.66017	349.22	0.58479	497.58	0.09312	46.55

without oxidative process, and also one reaction step with oxidative process. The last degradation stage (Zone III, with the mass loss of 10.03%) can be attributed to the oxidation of the organic matter (Gudmundssonand & Eliasson, 2006; Krochta, Hudson, & Tillin, 1987). Table 1 lists the values of characteristic (peak) temperatures (T_{p1}, T_{psh} and T_{p2}), degradation rates ($(d\alpha/dt)_{p1}$, $(d\alpha/dt)_{psh}$ and $(d\alpha/dt)_{p2}$) and the residual mass loss (Δm) for first and second peaks ("1" and "2") as well as for "shoulders" on DTG curves.

From Table 1 we can see that all characteristic temperatures, degradation rates and also residual mass loss values show the dependence on the heating rate (β). The corresponding temperatures and degradation rates belonging to observed reaction zones show an increase, with increasing of heating rate. This behavior is characteristic for the thermally stimulated processes in the solid state. It can also be seen that degradation rates at all of the observed heating rates for Peak 1 (belongs to Zone II (Fig. 1)) are significantly higher in comparison to degradation rates which belong to "shoulder" and Peak 2 (Table 1). From these results, we can conclude that in reaction Zone II, where non-oxidative process exists (within which most likely occurs carbonization that results in the release of gases (such as CO, CO_2 and probably compounds as CH_4 and C_2H_4) and char products) (Collinson & Thielemans, 2010; Fiedorowicz, Tomasik, & Lii, 2001; Soldi, 2005), the degradation rate is much higher than the rate of degradation in Zone III (Peak 2 in Table 1), which probably belongs to oxidation of the organic matter (maybe includes the oxidation of decomposed *Cassava* starch) (Tharanathan, 2005). The author believes that depending on the heating rate, the observed reaction stages (Zones II and III in Fig. 1) can be conjugated, and could cause the unification of reaction mechanisms multiple.

4.2. Isoconversional analysis

The obtained data were applied to isoconversional methods in order to determine the dependence of the apparent activation energy values on the degree of degradation ($E_a = E_a(\alpha)$). The conversion range between 0.05 and 0.95 was investigated. Fig. 2 shows $E_a = E_a(\alpha)$ dependence for the non-isothermal degradation of *Cassava* starch samples, calculated by the KAS and FR methods.

Results of KAS and FR analysis show that E_a value changes during the process (Fig. 2). It can be seen from Fig. 2 that both KAS and FR methods give similar values of E_a, and the same trend of E_a changes with increasing of α. At the very low values of α (in the range $0.05 \le \alpha \le 0.10$ and for the temperature up to 90 °C), we can observe the appearance of a low value of E_a (1.5–19.0 kJ mol^{-1}, taking into account both isoconversional methods). This conversion region corresponds to the free water molecules, which are present in starch granules. The apparent activation energy rapidly increases from 112.6 kJ mol^{-1} up to 426.5 kJ mol^{-1} (considering the values of E_a, calculated by KAS method), in conversion range $0.15 \le \alpha \le 0.25$ (250 °C $\le T \le$ 325 °C). The increasing behavior of E_a values with an increasing degree of degradation indicates a complex reaction mechanism, which includes a system of parallel and independent reactions. Already, in this conversion range, we can expect the start of starch degradation, i.e. degradation of amylose and amylopectin structures (characteristic average bond energies (D) in starch polymers are as follows: D(C—H) = 414.0 kJ mol^{-1}, D(CH—H) = 452.0 kJ mol^{-1}, D(H—H) = 435.0 kJ mol^{-1}, D(C—C) = 347.0 kJ mol^{-1}, D(C—O) = 360.0 kJ mol^{-1}, D(O—O) = 146 kJ mol^{-1} (Mukherji, Singh, & Kapoor, 2010)). Since the starch is a morphologically complex polymer, consisting of loose amorphous regions that are interspersed with highly regular crystalline regions, resulting from the formation of hydrogen bonds between the starch molecules (Smith, Zeeman, & Smith, 2005; Waigh et al., 1997), we can also expect that in the above-mentioned conversion range coming up the ruptures of hydrogen bonds and damage of starch crystalline structure, which leads to an increase in the value of E_a. This "action" breaks atomic and hydrogen bonds in the granules, which can reduce the size of crystalline region and creates the defects in crystalline structure, which can further accelerated the reactions that take place within considered conversion range (Table 1, column 3). It can be pointed out, that the double helices in the crystalline lamellae of amylopectin (formed by longer chains) require a much higher values of temperature (above 300 °C (Fig. 1)) to dissociate completely (Yamin, Lee, Pollak, & White, 1999). In addition, in considered α region, there is also the removal of bound water molecules impregnated into lamellar amylopectin structure, together with simultaneous early carbonization (Liu, Yu, Xie, Li, Chen, & Li, 2010) starting (Figs. 1 and 2). In a narrow conversion range $0.30 \le \alpha \le 0.40$ (325 °C $\le T \le$ 335 °C), we can see that the value of E_a do not vary significantly with α, so that in this region, E_a can be taken as a constant value ($\langle E_a \rangle^{KAS}$ = 838.4 kJ mol^{-1} and $\langle E_a \rangle^{FR}$ = 850.9 kJ mol^{-1}). In this region, the progressive carbonization process takes place in the absence of the variation in the apparent activation energy

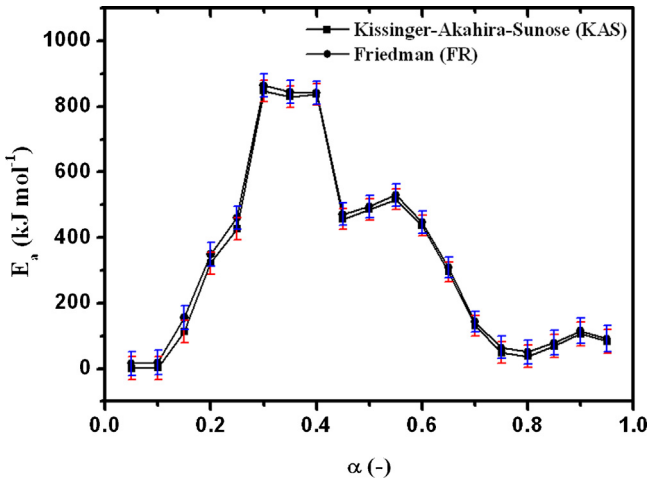

Fig. 2. Isoconversional dependences ($E_a = E_a(\alpha)$) for the non-isothermal thermo-oxidative degradation process of *Cassava* starch samples, calculated by the KAS (Kissinger–Akahira–Sunose) and FR (Friedman) methods.

values. However, in investigated conversion range, the gaseous products are formed (such as methane, carbon dioxide and water). Based on obtained high values of E_a (838.4 kJ mol^{-1}), we can also expect that there is a partial bond ruptures in the gaseous entities (for example, direct atomization of methane requires energy of 1665 kJ mol^{-1} (416.2 kJ mol^{-1} per C—H bond), while on the other hand, average bond energy for carbon–oxygen double bond (C=O) amounts 740 kJ mol^{-1} (Mukherji et al., 2010). Next conversion region, which corresponds to $0.45 \leq \alpha \leq 0.80$ (the temperature range 337 °C $\leq T \leq$ 430 °C, which includes "shoulder" on the right side of main peak in DTG curve up to 430 °C (Fig. 1)) shows a slight increase of E_a value (from 456.5 kJ mol^{-1} (α = 0.45) up to 486.3 kJ mol^{-1} (α = 0.50)), and then shows a decrease of E_a value (from 516.4 kJ mol^{-1} (α = 0.55) up to 37.5 kJ mol^{-1} (α = 0.80)). The obtained values of E_a, and behavior of the apparent activation energy with increasing of α, may indicate on a chain-end scission of C—C bonds (D(C—C) = 347 kJ mol^{-1}), generating more volatile products. The chain-end scission takes place at the gas–liquid interface in the reaction medium. The chain end degradation starts from the end of the chain and successively releases the monomer units. This type of degradation route is also known as depolymerization reaction, which involves successive release of monomer units from the chain ends (Price, Hourston, & Dumont, 2000). It can be pointed out, that the observed increase in E_a value, in narrow α range (from α = 0.45 to α = 0.55; T > 300 °C (Fig. 2)), may be ascribed to thermal condensation between hydroxyl groups of starch chains to form ether segments and lose water molecules and other small molecular species. Dehydration of neighboring hydroxyl groups in the glucose ring also occurred resulting in the formation of C=C (D(C=C) = 520 kJ mol^{-1}) (Mukherji et al., 2010) or breakdown of the glucose ring. Aldehyde groups were formed at the same time possibly as end groups if, and when the glucose ring was fractured. With increasing of temperature, the aromatic rings can be generated, such as substituted benzene and furan structures with either —CH_2— or —CH_2—O—CH_2— as main linkages between the aromatic groups. In addition, the carbonization reactions of investigated system at temperatures above 470 °C (for $\alpha \geq 0.85$; Fig. 2) probably lead to an increase in yield of aromatic carbon structures, and a decrease in yield of aliphatic carbons. Further increases in temperature will likely lead to generation of amorphous carbon structures. From observed dependence of E_a on α, the initial thermal reactivity significantly may depend on changes in the glucose units of starch and probably amylose content (Liu et al., 2010).

4.3. "Stationary point" kinetic analysis

Fig. 3 shows the Arrhenius-like plots evaluated by applying the stationary point method (Eq. (7)), for the Peak 1 (main), "shoulder (sh)" and Peak 2 of the DTG features, in the case of the non-isothermal degradation process of *Cassava* starch samples, in an air atmosphere.

From the slope ($-E_a/R$) of the obtained linear plots (Fig. 3) for all the observed reaction characteristics of the whole process, values of the apparent activation energy (E_a) were calculated. The following values of E_a were obtained: $E_{a,1}$ = 990.5 kJ mol^{-1} (Peak 1 (main)), $E_{a,sh}$ = 586.6 kJ mol^{-1} ("Shoulder" (sh)) and $E_{a,2}$ = 459.7 kJ mol^{-1}, respectively. The obtained values of E_a calculated by the stationary point method were slightly higher than those calculated by using KAS and FR isoconversional methods (Fig. 2). These differences were expected, because SP method gives only single value of E_a for the overall process, where T_p values can be very sensitive to the changes on the heating rate, and this is especially pronounced in the case of the complex processes that take place over several reaction stages.

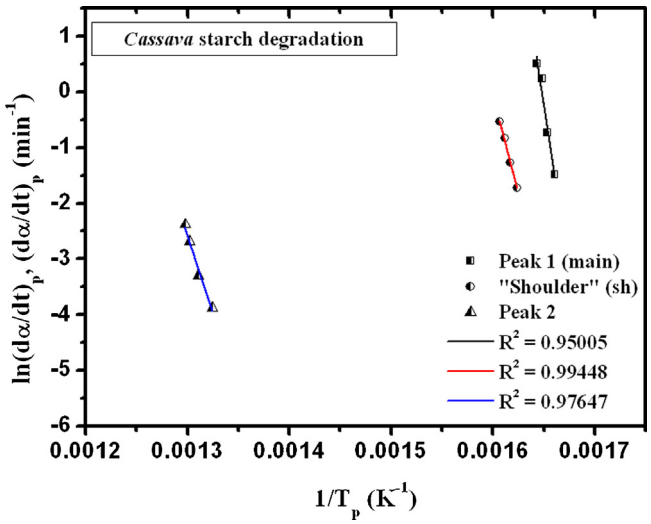

Fig. 3. The Arrhenius-like plots evaluated by applying the stationary point (SP) method, for Peak 1 (main), "shoulder (sh)" and Peak 2 on the corresponding DTG curves, in the case of the non-isothermal thermo-oxidative degradation process of *Cassava* starch samples.

4.4. Determination of the mechanism of the thermo-oxidative degradation

The E_a value was quite stable in a conversion range of 0.30–0.40 according to two isoconversional methods. Thus, the apparent activation energy value obtained by FR method (850.9 kJ mol^{-1}) was employed to calculate $y(\alpha)$ and $z(\alpha)$ functions. The dependence of $y(\alpha)$ function on degree of degradation (α), for the non-isothermal degradation of *Cassava* starch samples, at the different heating rates is shown in Fig. 4.

Each individual $y(\alpha)$ function is concave and has a clear maximum α_m at α = 0. These forms of $y(\alpha)$ functions are characteristic for kinetic models which rate-determining step is related to chemical reaction (reaction order (Rn) kinetic models), and also for kinetic models associated with diffusion phenomena (Málek et al., 2001). Based on the shape of $y(\alpha)$ functions (Fig. 4), we can conclude that the degradation process can be described by some kinetic models that belong to the groups of reaction order (RO(n)) or the diffusion

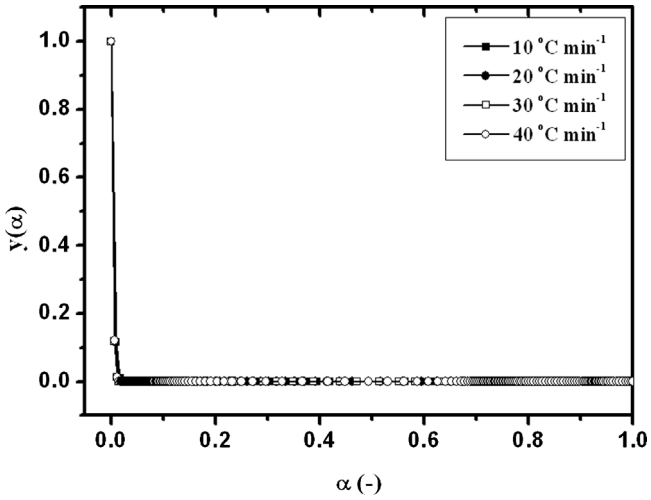

Fig. 4. The normalized $y(\alpha)$ functions for the thermo-oxidative degradation process of *Cassava* starch samples at: β = 10 °C min^{-1} (—■—), 20 °C min^{-1} (—●—), 30 °C min^{-1} (—□—) and 40 °C min^{-1} (—○—).

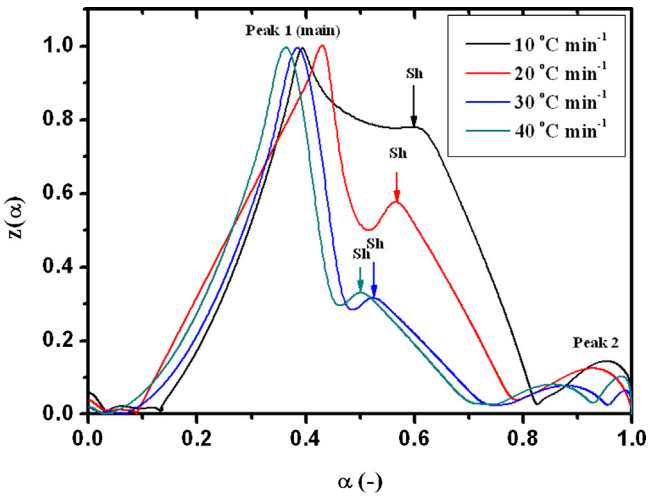

Fig. 5. The normalized $z(\alpha)$ functions for the thermo-oxidative degradation process of *Cassava* starch samples at: $\beta = 10\,^{\circ}C\,min^{-1}$ (—), $20\,^{\circ}C\,min^{-1}$ (▬), $30\,^{\circ}C\,min^{-1}$ (▬) and $40\,^{\circ}C\,min^{-1}$ (▬). At the same figure, the characteristic reaction zones designated by Peak 1 (main), "Sh" ("shoulder") and Peak 2 were also given.

(D) mechanisms. Fig. 5 shows the calculated $z(\alpha)$ functions at different heating rates, for considered degradation process of *Cassava* starch.

The shapes of the $z(\alpha)$ plots are practically variant with respect to heating rate. All $z(\alpha)$ plots clearly show three reaction zones designated with Peak 1 (main), "shoulder" (as "Sh") and Peak 2. The conversions, in which the $y(\alpha)$ and $z(\alpha)$ functions exhibit the maximum values (α_m and α_p^{∞}) for the different heating rates, are listed in Table 2.

For all reaction zones marked by the Peak 1 (main), "shoulder" and the Peak 2, the data in Table 2 which has been extracted from Fig. 5, show that α_p^{∞} values depend on the heating rate. These variances are corresponded to the variances in the calculated values of the apparent activation energies. Indeed, it can be concluded that kinetic process will not follow a single-step degradation model and the calculated values of E_a are really "*apparent*" values and may differ from the actual values. Since the obtained values of α_p^{∞} (Table 2) in all reaction zones are not equal to 0.632, 0.704, 0.776 and 0.834 (as the characteristic values for JMA (Johnson–Mehl–Avrami) (Johnson & Mehl, 1939; Avrami, 1939) model and D3, D4 and D2 diffusion models, respectively), the investigated degradation process can be described by the reaction order model (RO($n \neq 1$)), with different values of n. The data presented in Table 2 require further discussion. According to parameter α_p^{∞}, the kinetic model can be characterized and consequently reaction order n can be calculated (only if it is assumed that the process is subject

Table 2
The conversions, in which $y(\alpha)$ and $z(\alpha)$ curves exhibit the maximums (α_m and α_p^{∞}) (designated by peak 1 (main), "shoulder" (as "Sh") and peak 2) for the different heating rates.

Heating rate ($^{\circ}C\,min^{-1}$)	10	20	30	40
Peak 1 (main)				
α_m	0	0	0	0
α_p^{∞}	0.394	0.437	0.388	0.367
"Shoulder (Sh)"				
α_m	0	0	0	0
α_p^{∞}	0.777	0.567	0.525	0.500
Peak 2				
α_m	0	0	0	0
α_p^{∞}	0.951	0.926	0.873	0.845

Table 3
The values of reaction orders (n) for the observed reaction zones (peak 1 (main), "shoulder (Sh)" and peak 2), calculated by Eqs. (13) and (14), in the case of thermo-oxidative degradation of *Cassava* starch.

β ($^{\circ}C\,min^{-1}$)	10	20	30	40
Peak 1 (main)				
n (Eq. (13))	3.51	2.78	3.62	4.07
Average			3.49	
"Shoulder (Sh)"				
n (Eq. (13))	0.42	1.41	1.76	2.00
Average			1.40	
Peak 2				
n (Eq. (13))	0.06	0.10	0.19	0.24
Average			0.15	
Peak 1 (main)				
n (Eq. (14))	3.39	2.70	3.50	3.93
Average			3.38	
"Shoulder (Sh)"				
n (Eq. (14))	0.41	1.36	1.68	1.91
Average			1.34	
Peak 2				
n (Eq. (14))	0.05	0.10	0.18	0.23
Average			0.14	

to RO($n \neq 1$) model), from the following equation (Montserrat, Málek, & Colomer, 1998):

$$\alpha_p^{\infty} = 1 - n^{1/(1-n)} \tag{13}$$

Using this equation, the reaction order (n) can be calculated by an iterative calculation procedure. Values of n calculated by Eq. (13) for observed reaction zones at different β's are listed in Table 3.

It can be seen from Table 3 that the obtained values of n deviate from the first order reaction, and these values lie in the ranges $n = 2.78$–4.07 (Peak 1), $n = 0.42$–2.00 ("Shoulder") and $n = 0.06$–0.24 (Peak 2). Except for Peak 1, in two other cases, the value of n increases, with increasing of heating rate (Eq. (13); Table 3). The reaction order ($n \neq 0$) for RO(n) kinetic models can be calculated iteratively using equation in the form (Málek, 1992):

$$\alpha_p = 1 - \left[1 + \frac{(1-n)}{n} x_p \pi(x_p)\right]^{1/(n-1)} \tag{14}$$

Eq. (14) was derived originally by Gorbachev (Gorbachev, 1983) for $\pi(x_p) = 1/(x_p + 2)$, where $x_p = E_a/RT_p$. In order to calculate the reaction order at all observed heating rates for investigated reaction zones (Peak 1 (main), "Shoulder" and Peak 2), E_a values calculated by SP method were used. In order to test the validity of calculated values of reaction order by Eq. (14) and confirm the selected n-th order kinetic model ($f(\alpha) = (1-\alpha)^n$), values of n estimated by Eq. (14), are also listed in Table 3. From Table 3 we can see that there is very good agreement between the values of n, calculated using Eqs. (13) and (14), respectively.

4.5. Calculation of the pre-exponential factor

Knowing the value of the apparent activation energy and kinetic model, pre-exponential factor (A) can be calculated. Using the condition of maximum of thermo-analytical peak, the pre-exponential can be calculated by the following equation (Málek, 1992; Málek et al., 2001):

$$A = -\frac{\beta \cdot x_p}{T_p \cdot f'(\alpha_p)} \cdot \exp\,(x_p) \tag{15}$$

where $f'(\alpha_p) = df(\alpha_p)/d\alpha_p$.

Table 4
The values of $f(\alpha_p)$ and A, calculated by Eq. (15) for the observed reaction zones (peak 1 (main), "shoulder (Sh)" and peak 2), in the case of thermo-oxidative degradation of *Cassava* starch.

β (°C min^{-1})	Peak 1 (main)		"Shoulder (Sh)"		Peak 2	
	$f(\alpha_p)$	A (min^{-1})	$f(\alpha_p)$	A (min^{-1})	$f(\alpha_p)$	A (min^{-1})
10	−1.02085	2.669×10^{86}	−0.99295	1.079×10^{50}	−0.94942	6.541×10^{31}
20	−1.01539	2.326×10^{86}	−0.99812	1.308×10^{50}	−1.09103	5.233×10^{31}
30	−1.01733	1.819×10^{86}	−1.00084	1.351×10^{50}	−1.02868	5.004×10^{31}
40	−1.02267	1.270×10^{86}	−0.99528	1.253×10^{50}	−0.97734	5.455×10^{31}
Average	–	2.021×10^{86}	–	1.248×10^{50}	–	5.558×10^{31}

Table 4 shows the values of $f(\alpha_p)$ and A, calculated by Eq. (15), for investigated reaction zones (Peak 1 (main), "Shoulder" and Peak 2), in the case of thermo-oxidative degradation of *Cassava* starch samples.

As can be seen from Table 4, a very high values of pre-exponential factors (A) were obtained for all reaction zones, especially in the case of Peak 1. Values of pre-exponential factor for a solid phase reactions are expected to be in a wide range (six or seven orders of magnitude), even after the effect of surface area is taken into account. For the first order reactions, A may vary from 10^5 to 10^{17} min^{-1}, while for reactions which occur with $n \gg 1$ (large deviation from the first-order kinetics, as in the case for reaction under Peak 1 zone) the magnitude of pre-exponential factor can reach tens of potency in magnitude. High values of A usually indicate a formation of "loose" complexes in the system (Viswanathan, 2008; Forst, 1966). The formation of these complexes probably occurs in stages ascribed to "Peak 1" and "shoulder" (Table 4). In reaction stage attributed to Peak 2 (Table 4), the formation of such complexes is reduced in intensity, and minimizes at the end of the whole degradation process. In addition, high values of pre-exponential factor at the considered heating rates, for reaction zones attached with Peak 1 and "shoulder" (Table 4), indicate a quite number of degradation sites for investigated sample. It should be noted that based on results presented in Table 4, the continuous change of pre-exponential factor can be expected in air, taking into account the competitive oxidative reactions. These reactions emerge due to the possible new routes of oxidation, because new degradation centers can appear with the competitive reactions.

4.6. The interpretation of degradation mechanism

The routes of by which polymers degrade and that result in evolution of volatile products with an accompanying mass change, can be categorized into four main mechanisms, such as: main-chain scission, side group scission, elimination and depolymerization. Cyclization and cross-linking rarely result in any change of sample mass unless they occur in conjunction with the first four mechanisms, and are not detected by thermogravimetry (Chiu, 1987). For main reaction zone, the average values of reaction order (n) calculated by Eqs. (13) and (14) are 3.49 and 3.38 (Table 3), which indicate that in this stage, the degradation process is very complex and the system is more difficult to be degraded, and the more apparent activation energy is required during this stage of the process. This approach implies that cleavage of the first bonds will not immediately result in evaporation and, thus, this consideration may indicates an initiation period with a comparatively low conversion rate. In general, following this initiation period, the conversion rate first increases until it reaches a maximum and then decreases due to a decrease of the available number of bonds. Due to the complex nature of this degradation stage, its kinetics is not possible to be described with zero, first or second order kinetics. The complex nature of this degradation stage is reflected also through the fact that it was found, that for reactions with reaction order $n > 2.00$, the values of the pre-exponential factors obey to Gamma distribution (Capart, Khezami, & Burnham, 2004). For the reaction zone described by Peak 1, the mechanism of the process probably occurs through the series of competitive reactions, which includes depolymerization (which can be explained by the chain scission of the glycosidic linkage of polysaccharide), where occur through free radical mechanism (in this type of degradation, molecular weight of the biopolymer decreases slowly and large quantity of the monomer is liberated simultaneously), and subsequent decomposition of amylopectin and amylase degradation products. High value of reaction order, for this reaction zone (Table 3) (high orders in process description when, at least theoretically, the reaction order should not exceed 2) can be explained with a "lumped" model (Stolarek & Ledakowicz, 2005), which implies that the free radicals simultaneously attack both linear and branched molecular forms of the starch. Oxygen with free radicals R·, may create an active form ROO· which can with RH leads to appearance of ROOH + R·, who still participates in the process cycles. In this zone, like other polysaccharide, gaseous productions could include CO, CO_2, CH_4, H_2O, C_2H_4, and CH_2O (Soares, Lima, Oliveira, Pires, & Soldi, 2005). Probably the presence of CO, CO_2 and carbonyl compounds confirms that the scission of glycosidic linkages and strong bonds in backbone of starch taking place (Fig. 2). In next reaction zone ("substage") characterized by "shoulder", with mechanism described with average values of reaction order as $n = 1.40$ (=1.34) (Table 3), starch structure is disintegrated and highly cross-linked system was probably formed. After that, thermal reactions of investigated system followed the mechanism of cross-linking and decomposition of the formed levoluglucosan and furfural, where volatile products are safely released. In latter stage (Peak 2), the process occur through the mechanism with reaction order smaller than unity ($n = 0.15$ (Eq. (13)) and $n = 0.14$ (Eq. (14)) (Table 3)). Given that the value of n is very close to zero value, in this case the value of n can be approximated with zero-order kinetics. A zero-order reaction proceeds at a rate that is independent of reactant concentration. Increasing or decreasing the concentration of reactants will not speed up or slow down the reaction, respectively. This means, that the rate of reaction is equal to rate constant (k) of that reaction. In considered reaction zone (Peak 2), degradation proceeds through the carbonization reactions of studied system, at temperatures above 450 °C which probably increases the concentration of aromatic carbon compounds, and where we can expect here that concentration of aliphatic carbons decreases. Also, at even higher temperatures, in the range 580–600 °C, the probably formed conjugated aromatic structures in mentioned temperature range (Zhang, Looney, Solomon, & Whittaker, 1997), can generate the amorphous carbon structures. This assumption is justified if we take into account the obtained low value of E_a (almost three times lower value of E_a, than obtained values for E_a, in previous degradation stage (Fig. 2)). This amorphous carbon structures can easily burns in oxidative (air) atmosphere and thus facilitates the *Cassava* starch thermal degradation. This is sustained by lower apparent activation energy, where reactions occur with a zero-order

Table 5
The kinetic parameters obtained by the nonlinear least squares method, for the thermo-oxidative degradation of *Cassava* starch.

β (°C min^{-1})	10	20	30	40
Peak 1				
n [a]	3.42 (.10)	2.78 (.08)	3.61 (.04)	3.98 (.12)
E_a (kJ mol^{-1}) [a]	989.6 (5.3)	986.9 (4.2)	987.1 (2.1)	986.4 (2.8)
A (min^{-1}) [a]	1.501×10^{85}	4.201×10^{85}	6.933×10^{85}	5.022×10^{85}
fit (%)	7.68 (.07)	3.57 (.05)	4.35 (.11)	3.60 (.09)
"Shoulder (Sh)"				
n [a]	0.56 (.15)	1.42 (.16)	1.65 (.06)	1.98 (.05)
E_a (kJ mol^{-1}) [a]	582.8 (6.7)	583.6 (8.3)	588.1 (7.8)	589.7 (6.1)
A (min^{-1}) [a]	1.102×10^{49}	1.861×10^{49}	2.152×10^{49}	1.050×10^{49}
fit (%)	4.67 (.06)	5.01 (.02)	5.31 (.03)	4.82 (.06)
Peak 2				
n [a]	0.09 (.00)	0.12 (.02)	0.20 (.04)	0.27 (.04)
E_a (kJ mol^{-1}) [a]	461.8 (2.9)	460.3 (3.2)	457.9 (8.6)	462.1 (7.7)
A (min^{-1}) [a]	7.681×10^{30}	1.227×10^{30}	1.390×10^{30}	1.525×10^{30}
fit (%)	3.11 (.03)	3.69 (.05)	4.79 (.07)	4.18 (.14)

[a] Average values (av) of kinetic parameters ($E_{a,av}$, A_{av} and n_{av}) are presented in Fig. 6.

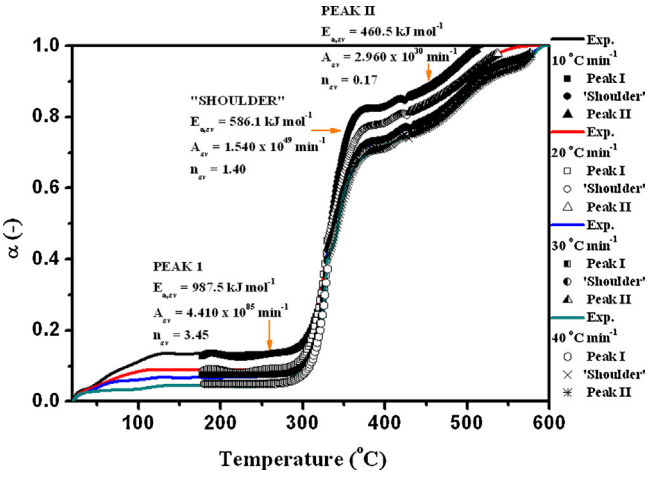

Fig. 6. The comparison between experimentally obtained non-isothermal α–T curves (lines), and calculated α–T curves (symbols) obtained by nonlinear least squares method, for the thermo-oxidative degradation process of *Cassava* starch samples. The average values of the kinetic parameters ($E_{a,av}$, A_{av} and n_{av}) are presented in the same figure.

mechanism, so that considered degradation stage is the slowest, compared to previous levels of degradation (Table 1). The rate of this degradation stage can be in the first approximation equals to the value of $(d\alpha/dt)_{p2}$, which are presented in Table 1 (for each of observed heating rate), so then we can infer $((d\alpha/dt)_{p2}) \equiv k_{p2}$.

Fig. 6 shows the comparison between experimentally obtained non-isothermal α–T curves (lines), and calculated α–T curves (symbols) obtained by nonlinear least squares method. The average values of kinetic parameters ($E_{a,av}$, A_{av} and n_{av}) are presented in the same figure.

It can be seen from Fig. 6 that there is a very good agreement between experimental and calculated non-isothermal conversion curves at all considered heating rates (β). The estimated kinetic parameters (values of kinetic parameters together with corresponding standard deviations, calculated by NLE method are listed in Table 5; almost negligible standard deviations at each of considered heating rates were obtained; the results indicate invariant the goodness of fit at different heating rates, and same results consequently imply the reliability of evaluated kinetic parameters as well as function $f(\alpha)$) are in good agreement with values of kinetic parameters derived using kinetic methods presented in this paper.

5. Conclusions

Thermo-oxidative degradation process of *Cassava* starch samples was investigated by thermogravimetric analysis (TGA) and derivative thermogravimetry (DTG) at the different heating rates (10, 20, 30 and 40 °C min^{-1}). It was established that degradation process proceeds through three main degradation stages with one additional sub-stage attached to the second degradation stage. First stage includes liberation of water molecules and other small molecular species. Second stage comprises the series of competitive reactions, which includes depolymerization (which can be explained by the chain scission of the glycosidic linkage of polysaccharide), where occur through free radical mechanism, and subsequent decomposition of amylopectin and amylase degradation products. It was explained that mechanism of process in this stage can be explained by the introduction of "lumped" model. The last reaction stage includes intensive carbonization reactions where the amorphous carbon structures were formed. It was found that identified degradation stages are characterized by specific values of reaction orders. The nonlinear least squares method was confirmed the reliability of evaluated kinetic parameters and also the function of reaction mechanism.

Acknowledgment

The author would like to thank the Ministry of Science and Environmental Protection of Serbia, for financial support of this research under the Project 172015.

References

Adnađević, B., Janković, B., Kolar-Anić, L. J., & Minić, D. (2007). Normalized Weibull distribution function for modeling the kinetics of non-isothermal dehydration of equilibrium swollen poly(acrylic acid) hydrogel. *Chemical Engineering Journal, 130*, 11–17.

Akahira, T., & Sunose, T. (1971). Method of determining activation deterioration constant of electrical insulating materials. *Chiba Institute of Technology, 16*, 22–31.

Avrami, M. (1939). Kinetics of phase change. I. General theory. *Journal of Chemical Physics, 7*, 1103–1112.

Ball, S. (1996). From glycogen to amylopectin: A model for the biogenesis of the plant starch granule. *Cell, 86*, 349–352.

Bogracheva, T. Y., Wang, Y. L., Wang, T. L., & Hedley, C. L. (2002). Structural studies of starches with different water contents. *Biopolymers, 64*, 268–281.

Burnham, A. K., & Dinh, L. N. (2007). A comparison of isoconversional and model-fitting approaches to kinetic parameter estimation and application predictions. *Journal of Thermal Analysis and Calorimetry, 89*, 479–490.

Capart, R., Khezami, L., & Burnham, A. K. (2004). Assessment of various kinetic models for the pyrolysis of a microgranular cellulose. *Thermochimica Acta, 417*, 79–89.

Chiangga, S., Suwannasopon, S., & Trivijitkasem, N. (2012). Thermal degradation of biodegradable poly(butylene adipate-co-terephthalate)/starch blends. *Kasetsart Journal (Nature Science), 46*, 653–661.

Chiu, J. (1987). Thermogravimetry for chemical analysis of polymers. In J. Jr. Mitchell (Ed.), *Applied polymer analysis and characterization: Recent developments in techniques, instrumentation, problem solving* (pp. 175–212). Munich, Germany: Hanser.

Coats, A. W., & Redfern, J. P. (1964). Kinetic parameters from thermogravimetric data. *Nature*, *201*, 68–69.

Collinson, S. R., & Thielemans, W. (2010). The catalytic oxidation of biomass to new materials focusing on starch cellulose and lignin. *Coordination Chemistry Reviews*, *254*, 1854–1870.

FAO. (1994). Food outlook: Global information and early warning system on food and agriculture, Number 10 (pp. 21–24) Rome.

Fiedorowicz, M., Tomasik, P., & Lii, C. Y. (2001). Degradation of starch by polarised light. *Carbohydrate Polymers*, *45*, 79–87.

Forst, W. (1966). Thermal decomposition of azomethane. II. The unimolecular reaction on the quantum harmonic model. *Journal of Chemical Physics*, *44*, 2349–2360.

Friedman, H. L. (1964). Kinetics of thermal degradation of char-forming plastics from thermogravimetry. Application to a phenolic plastic. *Journal of Polymer Science Part C: Polymer Symposium*, *6*, 183–195.

Gorbachev, V. M. (1983). Some suggestions for improving the utilization of the function $g(\alpha)$ and $p(x)$ to identify the mechanism of a thermal transformation. *Journal of Thermal Analysis and Calorimetry*, *27*, 151–154.

Greenwood, C. T., & Milne, E. A. (1968). Starch degrading and synthesizing enzymes: A discussion of their properties and action pattern. In M. L. Wolfrom, & R. S. Tipson (Eds.), *Advances in carbohydrate chemistry and biochemistry* (pp. 281–366). Amsterdam, The Netherlands: Elsevier Inc.

Gudmundssonand, M., & Eliasson, A. C. (2006). Starch – physicochemical and functional aspects. In A. C. Eliasson (Ed.), *Carbohydrates in food* (2nd ed., Vol. 10, pp. 391–471). Boca Raton, FL/London, UK/New York, USA: CRC Press, Taylor & Francis Group, LLC.

Guinesi, L. S., da Róz, A. L., Corradini, E., Mattoso, L. H. C., Teixeira de Eliangela, M., & da S. Curvelo, A. A. (2006). Kinetics of thermal degradation applied to starches from different botanical origins by non-isothermal procedures. *Thermochimica Acta*, *447*, 190–196.

Gyulai, G., & Greenhow, E. J. (1973). Approximation of the temperature integral in the evaluation of thermoanalytical measurements. *Thermochimica Acta*, *6*, 239–244.

Ji, Y., Seetharaman, K., Wong, K., Pollak, L. M., Duvick, S., Jane, J., et al. (2003). Thermal and structural properties of unusual starches from developmental corn lines. *Carbohydrate Polymers*, *51*, 439–450.

Johnson, W., & Mehl, R. (1939). Reaction kinetics in processes of nucleation and growth. *Transactions of the Metallurgical Society of AIME*, *135*, 416–442.

Kissinger, H. E. (1957). Reaction kinetics in differential thermal analysis. *Analytical Chemistry*, *29*, 1702–1706.

Krochta, J. M., Hudson, J. S., & Tillin, S. J. (1987). Kinetics of alkaline thermochemical degradation of polysaccharides to organic acids. *American Chemistry Society Division of Fuel Chemistry*, *32*, 148–153.

Liu, X., Yu, L., Xie, F., Li, M., Chen, L., & Li, X. (2010). Kinetics and mechanism of thermal decomposition of cornstarches with different amylose/amylopectin ratios. *Starch/Stärke*, *62*, 139–146.

Málek, J. (1992). The kinetic analysis of non-isothermal data. *Thermochimica Acta*, *200*, 257–269.

Málek, J., Mitsuhashi, T., & Criado, J. M. (2001). Kinetic analysis of solid-state processes. *Journal of Materials Research*, *16*, 1862–1871.

MathWorks Inc., MATLAB®. (2012). The language of technical computing (a high-level language and interactive environment for numerical computation, visualization, and programming). http://www.mathworks.com/products/matlab/

Montserrat, S., Málek, J., & Colomer, P. (1998). Thermal degradation kinetics of epoxy-anhydride resins. I. Influence of a silica filler. *Thermochimica Acta*, *313*, 83–95.

Morita, H. (1956). Characterization of starch related polysaccharides by differential thermal analysis. *Analytical Chemistry*, *28*, 64–67.

Morita, H. (1957). Differential thermal analysis of some polyglucosans. *Analytical Chemistry*, *29*, 1095–1097.

Morrison, W. R., & Laignelet, B. (1983). An improved colorimetric procedure for determination apparent and total amylose in cereal and other starches. *Journal of Cereal Science*, *1*, 9–16.

Morrison, W. R., Law, R. V., & Snape, C. E. (1993). Evidence for inclusion complexes of lipids with V-amylose in maize rice and oat starches. *Journal of Cereal Science*, *18*, 107–109.

Mukherji, S. M., Singh, S. P., & Kapoor, R. P. (2010). Structure and bonding. In R. Dass (Ed.), *Organic chemistry, Vol. I* (2nd ed., pp. 1–22). Darya Ganj, New Delhi, India: New Age International Publishers.

Pielichowski, K., Tomasik, P., & Sikora, M. (1998). Kinetics of gelatinization of potato starch studied by non-isothermal DSC. *Carbohydrate Polymers*, *35*, 49–54.

Pineda-Gómez, P., Coral, D. F., Ramos-Rivera, D., Rosales-Rivera, A., & Rodríguez-García, M. E. (2011). Thermo-alkaline treatment. A process that changes the thermal properties of corn starch. *Procedia Food Science*, *1*, 370–378.

Price, D. M., Hourston, D. J., & Dumont, F. (2000). Thermogravimetry of polymers. Encyclopedia of analytical chemistry. In R. A. Meyers (Ed.), *Encyclopedia of Analytical Chemistry* (pp. 8094–8105). Chichester, West Sussex, UK: John Wiley & Sons, Ltd.

Rahman, W. A. W. A., Sin, L. T., Rahmat, A. R., & Samad, A. A. (2010). Thermal behaviour and interactions of *Cassava* starch filled with glycerol plasticized polyvinyl alcohol blends. *Carbohydrate Polymers*, *81*, 805–810.

Senum, G. I., & Yang, R. T. (1977). Rational approximations of the integral of the Arrhenius function. *Journal of Thermal Analysis and Calorimetry*, *11*, 445–449.

Smith, A. M., Zeeman, S. C., & Smith, S. M. (2005). Starch degradation. *Annual Review of Plant Biology*, *56*, 73–98.

Soares, R. M. D., Lima, A. M. F., Oliveira, R. V. B., Pires, A. T. N., & Soldi, V. (2005). Thermal degradation of biodegradable edible films based on xanthan and starches from different sources. *Polymer Degradation and Stability*, *90*, 449–454.

Soldi, V. (2005). Stability and degradation of polysaccharides. In S. Dumitriu (Ed.), *Polysaccharides – structural diversity and functional versatility* (2nd ed., pp. 395–411). New York, USA: Marcel Dekker/CRC Press.

Soni, P. L., Sharma, H., Dun, D., & Gharia, M. M. (1993). Physicochemical properties of *Quercus leucotrichophora* (Oak) starch. *Starch/Stärke*, *45*, 127–130.

Stolarek, P., & Ledakowicz, S. (2005). Pyrolysis kinetics of chitin by non-isothermal thermogravimetry. *Thermochimica Acta*, *433*, 200–208.

Swinkels, J. J. M. (1985). Sources of starch, its chemistry and physics. In G. M. A. van Beynum, & J. A. Roels (Eds.), *Starch conversion technology* (pp. 15–46). New York: Marcel Dekker Inc.

Tharanathan, R. N. (2005). Starch – value addition by modification. *Critical Reviews in Food Science and Nutrition*, *45*, 371–384.

Tian, Y., Xu, X., Xie, Z., Zhao, J., & Jin, Z. (2011). Starch retrogradation determined by differential thermal analysis (DTA). *Food Hydrocolloids*, *25*, 1637–1639.

Tonukari, N. J. (2004). Cassava and the future of starch. *Electronic Journal of Biotechnology*, *7*, 5–8.

Van den, B.C. (1981). *Vapour sorption equilibria and other water-starch interactions: A physico-chemical approach*. Wageningen Agricultural University. Ph.D. Thesis, 9–15.

Varhegyi, G., Antal, M. J., Szekely, T., & Szabo, P. (1989). Kinetics of the thermal decomposition of cellulose, hemicellulose and sugar-cane bagasse. *Energy & Fuels*, *3*, 329–335.

Viswanathan, B. (2008). Appropriateness of Arrhenius equation for kinetic analysis of solid state reactions. In *National workshop on thermal analsyis at IGCAR february, National Centre for Catalysis Research* Indian Institute of Technology, Madras, Chennai, India, (pp. 1–15).

Vyazovkin, S., & Wight, C. A. (1999). Model-free and model-fitting approaches to kinetic analysis of isothermal and nonisothermal data. *Thermochimica Acta*, *340/341*, 53–68.

Vyazovkin, S., & Wight, C. A. (1998). Isothermal and non-isothermal kinetics of thermally stimulated reactions of solids. *International Reviews in Physical Chemistry*, *17*, 407–433.

Waigh, T. A., Hopkinson, I., Donald, A. M., Butler, M. F., Heidelbach, F., & Riekel, C. (1997). Analysis of the native structure of starch granules with X-ray microfocus diffraction. *Macromolecules*, *30*, 3813–3820.

Yamin, F. F., Lee, M., Pollak, L. M., & White, P. J. (1999). Thermal properties of starch in corn variants isolated after chemical mutagenesis of inbred line B73. *Cereal Chemistry*, *76*, 175–181.

Zhang, X., Looney, M. G., Solomon, D. H., & Whittaker, A. K. (1997). The chemistry of novolac resins: 3 ^{13}C and ^{15}N NMR studies of curing with hexamethylenetetramine. *Polymer*, *38*, 5835–5848.